J Solid State Electrochem (2016) 20:273–283
DOI 10.1007/s10008-015-3034-1

ORIGINAL PAPER

Photoanodes on titanium substrates: one-step deposited $BiVO_4$ versus two-step nano-V_2O_5 films impregnated with Bi^{3+}

Murilo F. Gromboni[1] · Moisés A. Araújo[1] · Elizabeth Downey[2] · Frank Marken[2] · Lucia H. Mascaro[1]

Received: 25 June 2015 / Accepted: 1 September 2015 / Published online: 17 September 2015

Abstract One-step deposition of photoelectrochemically active $BiVO_4$ (monoclinic) from a polyethylene glycol (PEG300) precursor paint onto titanium substrates is demonstrated to lead to more complex multioxide phase films. Photocurrents in 0.5 M Na_2SO_4 remain relatively low when compared to those reported on tin-doped indium oxide (ITO) substrates, possibly due to the effect of detrimental underlying titanium oxide phases or mixed phases. For comparison, the one-step deposition is demonstrated also for the direct formation of V_2O_5 nanocrystalline films, which also exhibited low photoelectrochemical activity. Impregnation of nanocrystalline V_2O_5 with aqueous Bi^{3+} is shown to cause substantial recrystallization with formation of much more photoactive $BiVO_4$. In particular, on low-temperature (high surface area) nano-V_2O_5 (400 °C) and after further mild annealing at 400 °C much improved photoelectrochemical water oxidation activity (ca. 0.3 mA cm^{-2} at 1.0 V vs Ag/AgCl (KCl (3 M) at 0.1-W cm^{-2} xenon lamp radiation) is observed. This opens up a new mild temperature two-step route for $BiVO_4$ photocatalysts on practical titanium substrates.

Keywords Photovoltammetry · PEG · Nucleation · Titanium · Energy · Water splitting

✉ Frank Marken
F.marken@bath.ac.uk

[1] Department of Chemistry, Federal University of São Carlos, Rod. Washigton Luiz, km235, CEP 13565-905 São Carlos, SP, Brazil

[2] Department of Chemistry, University of Bath, Claverton Down, Bath BA2 7AY, UK

Introduction

Solar-driven water splitting requires (i) photoactive components for the charge separation step followed by (ii) effective conduction of one or both of the electron/hole charge carriers and (iii) effective surface reactions to give oxygen evolution at the photoanode as well as effective use of the photogenerated electron [1, 2]. Many materials are good at one or two of these requirements, but few allow the complete reaction sequence to occur in a single material without further material engineering. $BiVO_4$ has been identified as an excellent candidate material [3–5] for the anodic water splitting reaction (see Fig. 1) where holes are retained at the surface of the semiconductor to allow effective light-driven water oxidation to oxygen.

$BiVO_4$ bulk and surface-immobilized materials for film electrodes have been produced via a wide range of synthetic methods including traditional sol-gel synthesis [6], hydrothermal [7], sonochemical [8], spray deposition [9], vapor deposition [10], and aqueous/coprecipitation methods [11]. Most of the film devices have been produced on transparent substrates such as tin-doped indium oxide (ITO) to give very good photoelectrochemical current responses with IPCE values reported up to 70 % [12]. Additional modification has been demonstrated in the bulk with phosphate [13], lanthanum [14], and at the surface with Ir [15], Mo [16], Co [17], Ni [18], WO_3 [12], etc. to further increase the energy yield in the form of oxygen and electrons generated. The combination of a $BiVO_4$ photoanode with the organic TEMPO redox mediator has been proposed for biomass valorization [19]. Recently, amorphous TiO_2 buffer layer deposition (see Fig. 1; similar to that in dye sensitized solar cells [20]) has been proposed by Bard and coworkers to minimize recombination at the (ITO) substrate [21]. Both materials, $BiVO_4$

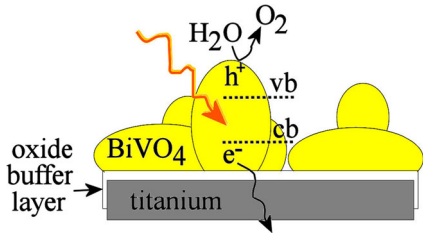

Fig. 1 Schematic drawing of the light absorption, followed by charge separation, conduction of holes to the surface and electrons into the bulk (toward electrode), and multielectron oxygen generation. The case of an underlying oxide buffer layer, here TiO_2 on a titanium substrate is introduced

and TiO_2, have been suggested to share a similar conduction band energy level [22] to allow transport of electrons away into the metallic electrode although this may strongly depend on morphology. On the other hand, TiO_2 itself has been the subject to intense study as a candidate UV-photoanode because it offers a low-cost technology and it exhibits faster electron transfer/degradation rates compared with most other oxide photocatalysts [23]. The $BiVO_4$-TiO_2 junction has been studied in a few reports [24, 25] as an interesting candidate structure for water splitting and in enhanced photocatalytic decomposition of organic pollutants [26]. Ho-Kimura et al. [27] observed that higher stability films were obtained and the photocurrent was increased by a factor four using the nanostructured junction compared to bare $BiVO_4$. The fabrication challenge of depositing $BiVO_4$ directly onto titanium substrates is new and considered in this report.

We have recently proposed a practical "one-step" synthesis approach based on a polyethylene glycol (here PEG300 as a benign and nonvolatile solvent) paint containing Bi(III) nitrate and ammonium meta-vanadate [28]. The paint was applied to ITO-coated glass and conditions optimized to give good water oxidation performance. The paint method is versatile and potentially applicable for other types of substrates such as titanium. Taking into account the improvement in photocatalytic properties reported in the literature, it appears reasonable to combine TiO_2 and $BiVO_4$ and to explore the $BiVO_4$ film growth directly on bulk (industrial) titanium substrates. Titanium as a robust engineering material offers many advantages over surface conducting glass; however, the effects of additional interfacial oxide phases could introduce more complexity. In this report, we investigate the one-step $BiVO_4$ synthesis in conjunction with the use of cheap titanium substrates to replace the lower melting ITO-coated glass substrates. Initial problems with detrimental oxide phases were overcome by first making a film of nano-V_2O_5 on titanium followed by impregnation with Bi^{3+} and annealing. The resulting process works well even under milder annealing conditions (at 400 °C) as an additional benefit.

Experimental

Reagents

Chemical reagents used in the synthesis were PEG-300, ammonium metavanadate, bismuth(III) nitrate, and nitric acid (all Sigma-Aldrich, ACS purity). The supporting electrolyte in photovoltammetric measurements was aqueous 0.5 mol dm^{-3} di-sodium sulfate. Aqueous solutions were prepared from deionized water from a MilliQ system (18 MΩ cm at 22 °C).

Instrumentation

X-ray diffraction data were obtained using a Shimadzu diffractometer model XRD-6000, in θ–2θ mode, from 5° to 80°, rate 1° s^{-1} and electrode voltage 30 kV. The electron microscopy images (SEM/FEG) and EDS spectra were obtained using a FEI microscope Inspect S50. Photoelectrochemical measurements in 0.5 mol dm^{-3} Na_2SO_4 were performed with an electrochemical cell contained in a 2-in. quartz window and an optical path of 5 cm, which was illuminated by a light source from Newport model 66902, equipped with a xenon lamp with 150-W nominal powers. The intensity used during the experiments was 0.1 W cm^{-2} in the front of cell. The voltammetric measurements were obtained using a potentiostat/galvanostat AUTOLAB PGSTAT30. As reference electrode Ag/AgCl/KCl 3 mol dm^{-3} and a

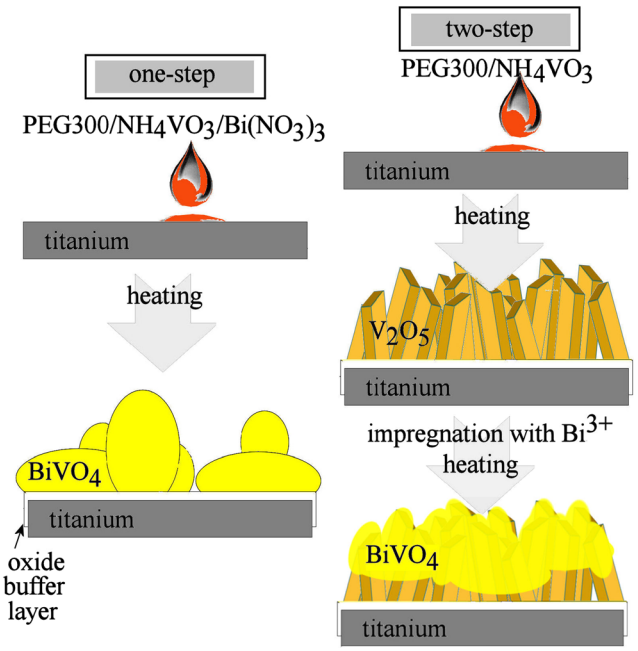

Fig. 2 Schematic drawing of the "one-step" deposition of $BiVO_4$ and the "two-step" deposition of $BiVO_4$ on titanium substrates

platinum plate (2 cm^2) as counter electrode. In these measurements, the in-active face of the titanium substrate without the photoactive film was insulated using a mixture of nitrocellulose resin and epoxy resin.

Electrode fabrication

The titanium substrates were cut with the dimensions 1.0 cm× 1.5 cm. A mechanical pretreatment was performed on

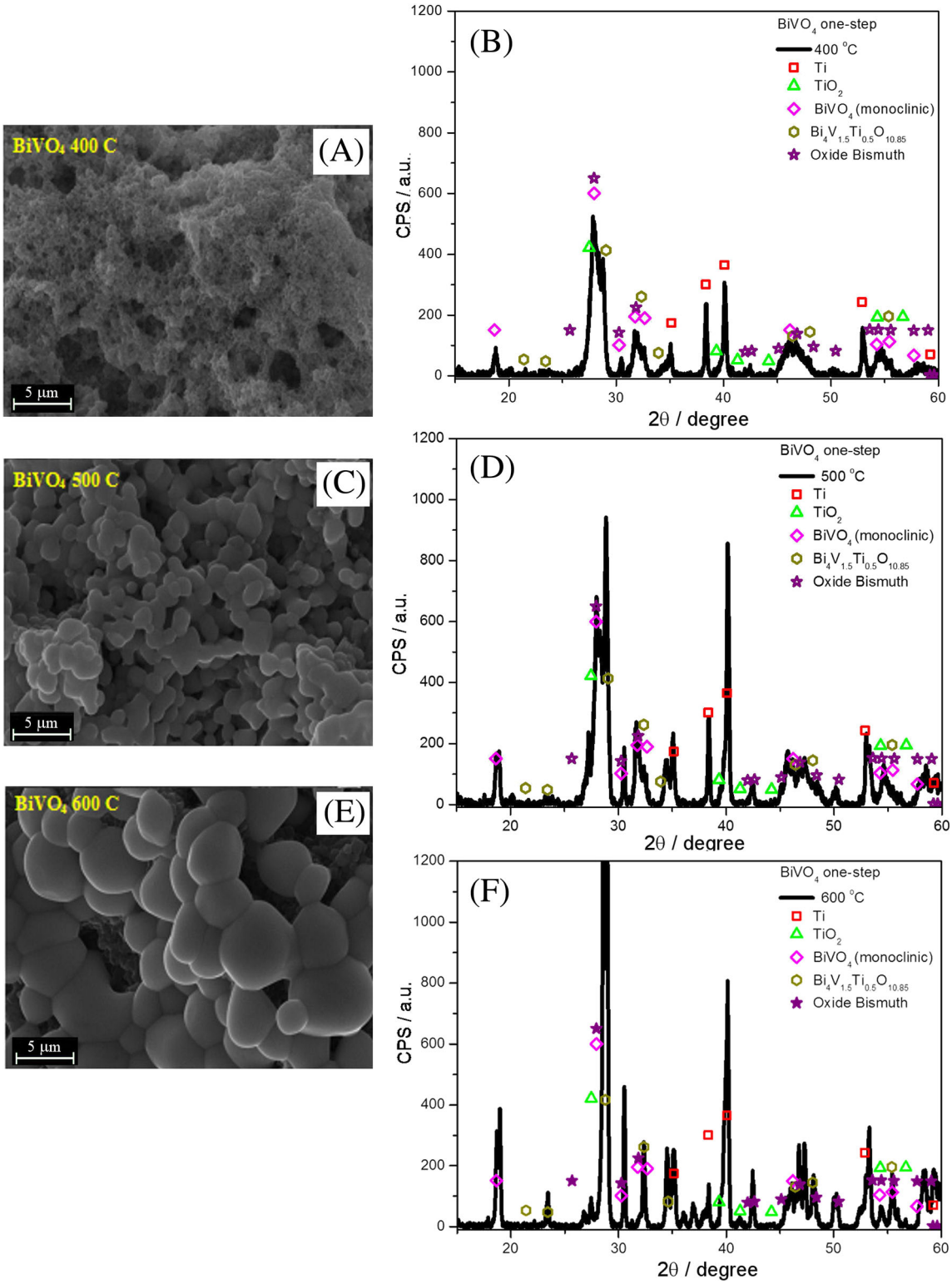

Fig. 3 **a**, **c**, **e** Scanning electron microscopy (SEM) images of "one-step" $BiVO_4$ films obtained at calcination temperatures of 400, 500, and 600 °C. **b**, **d**, **f** XRD data for 400, 500, and 600 °C samples

titanium substrates using sand blasting. Then, substrates were washed in deionized water and boiled for 20 min in 10 % oxalic acid solution. Finally, they were washed with deionized water and dried at 120 °C for 10 min. The paint used to obtain the active $BiVO_4$ (monoclinic) films was prepared by mixing (A) a suspension of 200 mg NH_4VO_3 in 2 mL PEG300 and (B) 414 mg $Bi(NO_3)_3$ in 2 mL PEG300. After 20-min sonication, a uniform paint was obtained. The paint for preparation of nanocrystalline V_2O_5 was prepared as a suspension of 125 mg NH_4VO_3 in 2.5 mL of PEG300 with 20-min sonication (at 10 °C). For coating of the titanium substrates an aliquot part of 5 μL cm^{-2} per layer of prepared suspension was applied. The samples were obtained with five consecutive layers with a 10-min drying step at 400 °C applied for each layer. Next, samples were calcined for 60 min at different temperatures (400, 500, and 600 °C). After calcination, the oven was turned off and the samples slowly cooled to ambient conditions. The impregnation of the samples of nanocrystalline V_2O_5 with aqueous Bi^{3+} was achieved by immersion (10, 20, 30, 60, or 120 min with agitation) into 10 mM $Bi(NO_3)_3$ in aqueous 0.01 M HNO_3 (Fig. 2).

Results and discussion

One-step deposition of $BiVO_4$ films on titanium substrates

Films of $BiVO_4$ prepared by the one-step method on titanium exhibit the characteristic yellow color of $BiVO_4$. Scanning electron microscopy (SEM) images of samples reveal a gradual increase in grain size with calcination temperature (Fig. 3). Products formed at 400 °C appear nanograined and diffuse when compared to particles formed at 500 °C (ca. 2 μm diameter) and at 600 °C (ca. 5 μm diameter).

X-ray crystallographic (XRD) investigation of the film deposits reveals the presence of $BiVO_4$ as well as underlying titanium and other mixed oxide phases (Fig. 3). In the XRD analysis for the sample prepared at 400 °C, diffraction peaks for the monoclinic bismuth vanadate phase are not clearly resolved. For samples prepared at 500 and 600 °C, much clearer peaks for monoclinic $BiVO_4$ are resolved. However, all samples showed the presence of additional oxide phases. At temperatures of 400 to 500 °C, the formation of phases of bismuth oxide ($Bi_2O_{2.5}$) and bismuth titanium vanadium oxide ($Bi_{3.8}V_{1.5}Ti_{0.7}O_{10.85}$) is observed. At 600 °C, the bismuth titanium vanadium oxide is observed.

Energy-dispersive fluorescence spectra (EDS) were obtained under SEM conditions with 15-KeV beam energy (see Table 1). All samples appeared slightly Bi-rich with the sample obtained at 400 °C showing the highest amount of Bi in the composition (consistent with less oxide overage). The average atom% ratios are Bi/V=1.22, 1.28, and 1.17 for samples prepared at temperatures of 400, 500, and 600 °C, respectively.

Table 1 Energy-dispersive fluorescence (EDS) data obtained under SEM conditions with 15-KeV electron beam energy for "one-step" $BiVO_4$ samples on titanium

T (°C)	Region	Atom %			
		V	Bi	O	Ti
400	1	4.38	6.00	65.02	24.60
	2	6.11	7.97	65.44	20.48
	3	7.44	7.84	64.41	20.31
	Average	5.98	7.27	64.96	21.80
500	1	5.64	7.66	63.31	23.39
	2	6.25	7.70	64.89	21.16
	3	4.67	5.84	64.61	24.88
	Average	5.52	7.07	64.27	23.14
600	1	3.99	5.54	71.34	19.13
	2	4.49	4.23	74.22	17.06
	3	3.40	4.13	73.65	18.82
	Average	3.96	4.63	73.07	18.34

In the voltammetric experiments (Fig. 4), the $BiVO_4$ film electrodes exhibit a broad reduction peak with a corresponding oxidation peak centered at 0.3 V versus Ag/AgCl (KCl 3 M). This reduction and re-oxidation is consistent with V(V) being reduced to V(IV) at the surface of the $BiVO_4$ deposit. There is a trend of the low-temperature sample (prepared at 400 °C) showing higher current, consistent with the finer grains (Fig. 3) and consistent with better conductivity across the oxide buffer layer (which is expected to thicken at higher temperatures).

When investigating phototransients (Fig. 4b), the sample prepared at 400 °C clearly shows the highest photo response (onset at 0.0 V vs Ag/AgCl (KCl 3 M)), but the overall magnitude of the current, ca. 30 μA cm^{-2} at 1.0 V versus Ag/AgCl (KCl 3 M) is low in comparison to similar electrodes prepared on tin-doped indium oxide substrates [27]. It is likely that the multilayer (multicomponent) structure with the underlying oxide buffer layer is detrimental under these conditions, in particular for the samples calcined at higher temperatures. In order to modify the buffer layer structure a "two-step" method is investigated next.

One-step deposition of nano-V_2O_5 films on titanium substrates

With photoelectrochemical $BiVO_4$ responses indicating poor performance in anodic water splitting on titanium substrates, it was decided to further simplify the synthesis and to explore the properties of nano-V_2O_5 as photoactive film on titanium. Visually, film of nano-V_2O_5 exhibit the typical brown color of V_2O_5. Figure 5 shows typical scanning electron micrographs (SEMs) for

the nanocrystalline V_2O_5 formed via one-step method with calcination at 400, 500, and 600 °C. Crazing of the film is evident with a very fine-grained product produced at 400 °C. At calcination temperatures of 500 °C ca. 0.2-μm-sized crystals are produced and at 600 °C, the crystal size is increased to typically 1–2 μm. EDS (not shown) confirms the presence of V and Ti. In XRD analyses (Fig. 5b, d, f) the orthorhombic V_2O_5, TiO_2, and titanium substrate are observed in all samples. The sample prepared at 600 °C contained the highest level of TiO_2 and possibly traces of tetragonal $TiVO_4$.

Electrochemical experiments were first performed for a sample of PEG300 only on a titanium substrate (Fig. 6a). A clear change with calcination temperature is observed with higher anodic currents for lower calcination temperature samples. This is consistent with oxide film growth passivating the 600 °C sample. The currents observed for the nano-V_2O_5-coated electrodes are significantly higher compared to those just for the substrate. A first reduction peak with a corresponding oxidation peak occurs centered at ca. 0.4 V versus Ag/AgCl (KCl 3 M). This electrochemical response is closely related to those observed for $BiVO_4$ (Fig. 4a) and therefore

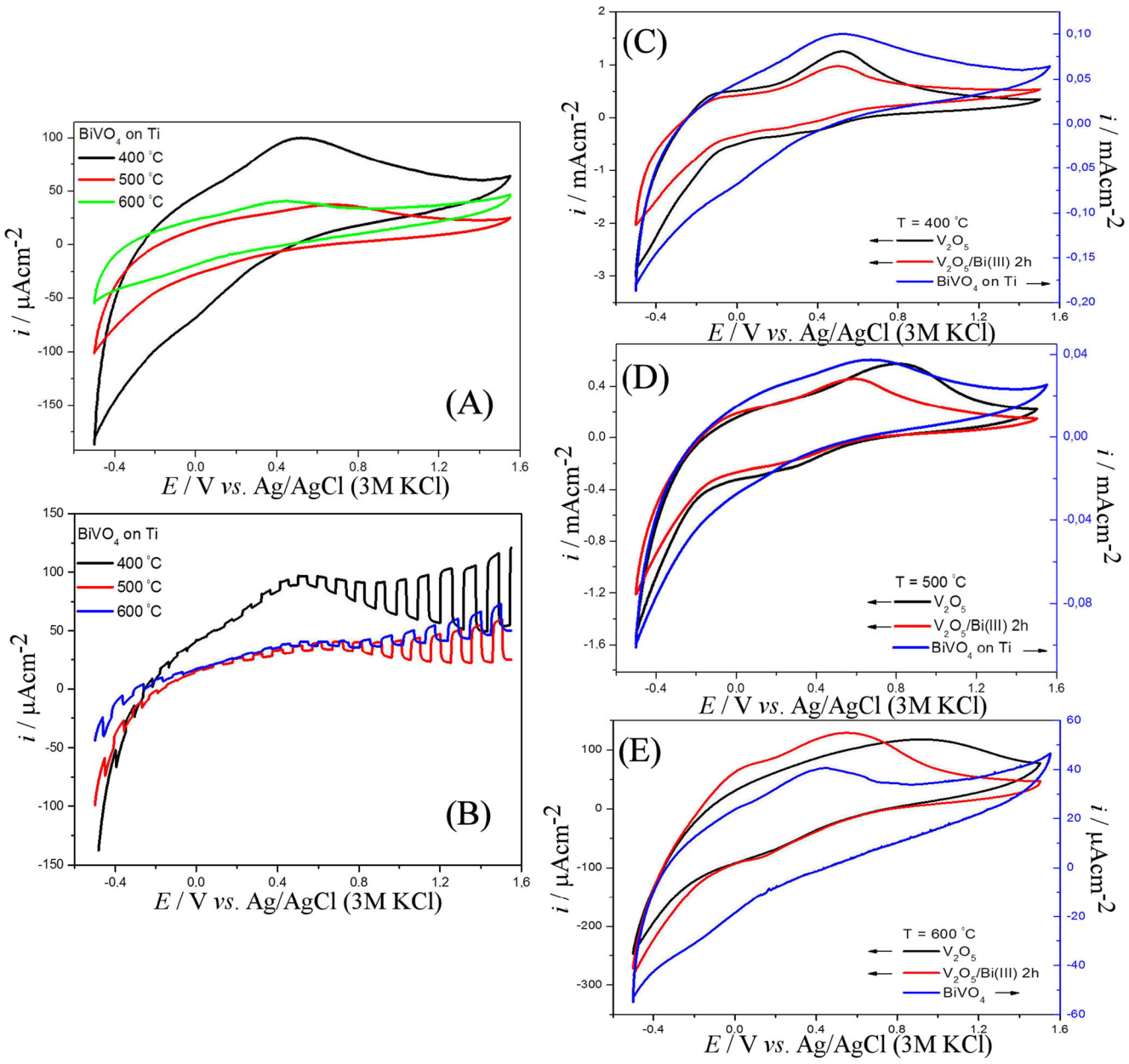

Fig. 4 **a** Cyclic voltammograms (0.5 mol dm^{-3} Na_2SO_4, third potential cycle shown; scan rate 20 mV s^{-1}) comparing one-step $BiVO_4$ film electrodes produced at 400, 500, and 600 °C. **b** As above, but with light pulses (only positive-going scan shown). **c**–**e** Cyclic voltammograms (0.5 mol dm^{-3} Na_2SO_4, third potential cycle shown; scan rate 20 mV s^{-1}) comparing one-step $BiVO_4$ film electrodes, nano-V_2O_5 film electrodes, and Bi^{3+}-impregnated film electrodes fabricated at **c** 400, **d** 500, and **e** 600 °C (note the change in scale)

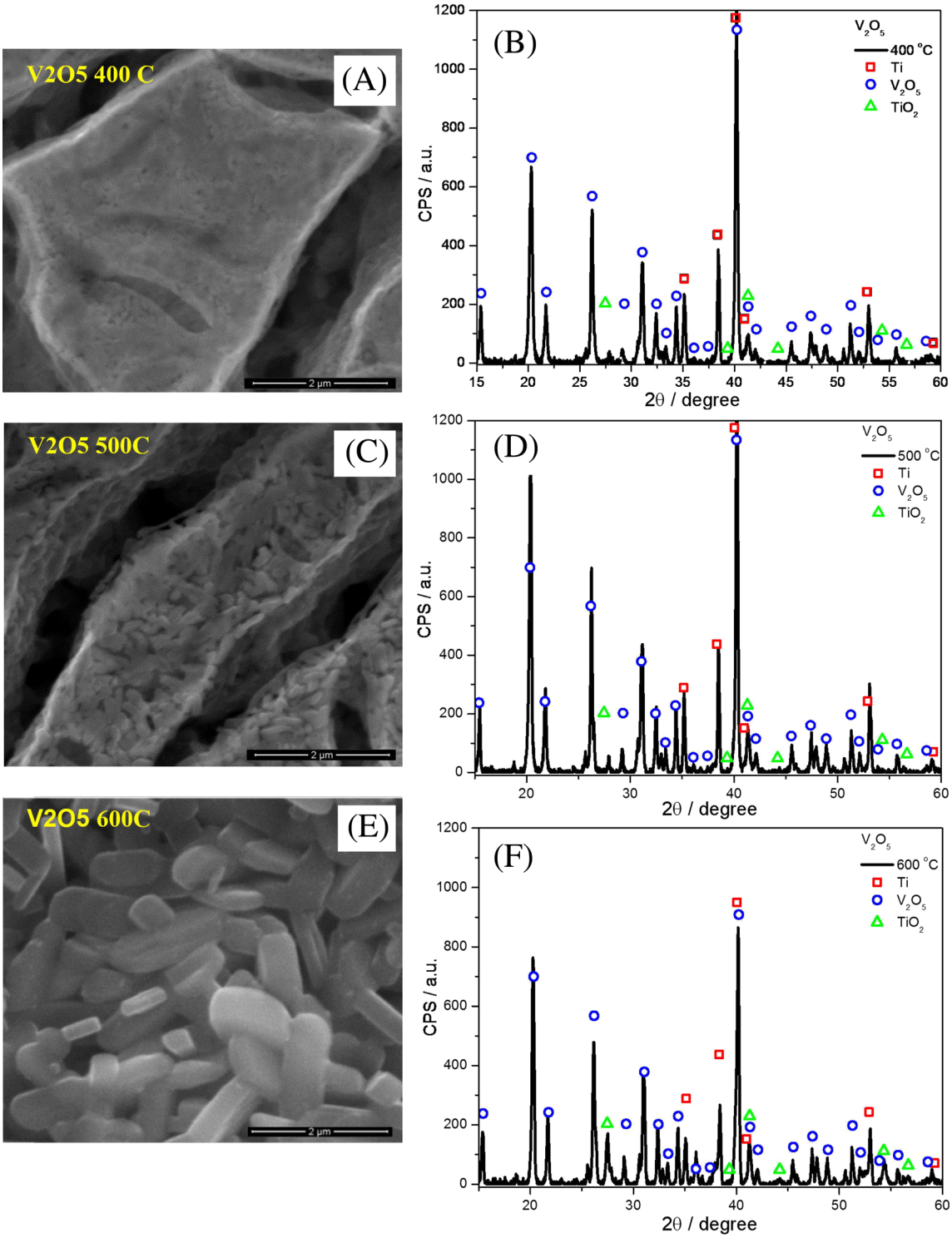

Fig. 5 **a**, **c**, **e** Scanning electron microscopy (SEM) images of "one-step" nano-V_2O_5 films obtained at calcination temperatures of 400, 500, and 600 °C. **b**, **d**, **f** XRD data for 400, 500, and 600 °C samples

assigned here to the V(V) to V(IV) reduction of the surface (compare similar observations in the literature [29]). A secondary reduction with onset at −0.2 V versus Ag/AgCl (KCl 3 M) is likely to be associated with the intercalation of cations into the V_2O_5 lattice. When comparing samples that were annealed at 400, 500, and 600 °C, again a clear trend is observed with higher annealing temperatures resulting in suppression of the Faradaic current for the V_2O_5 redox process. The two main reasons for this are (i) a decrease in V_2O_5 surface area at higher calcination temperatures and (ii)

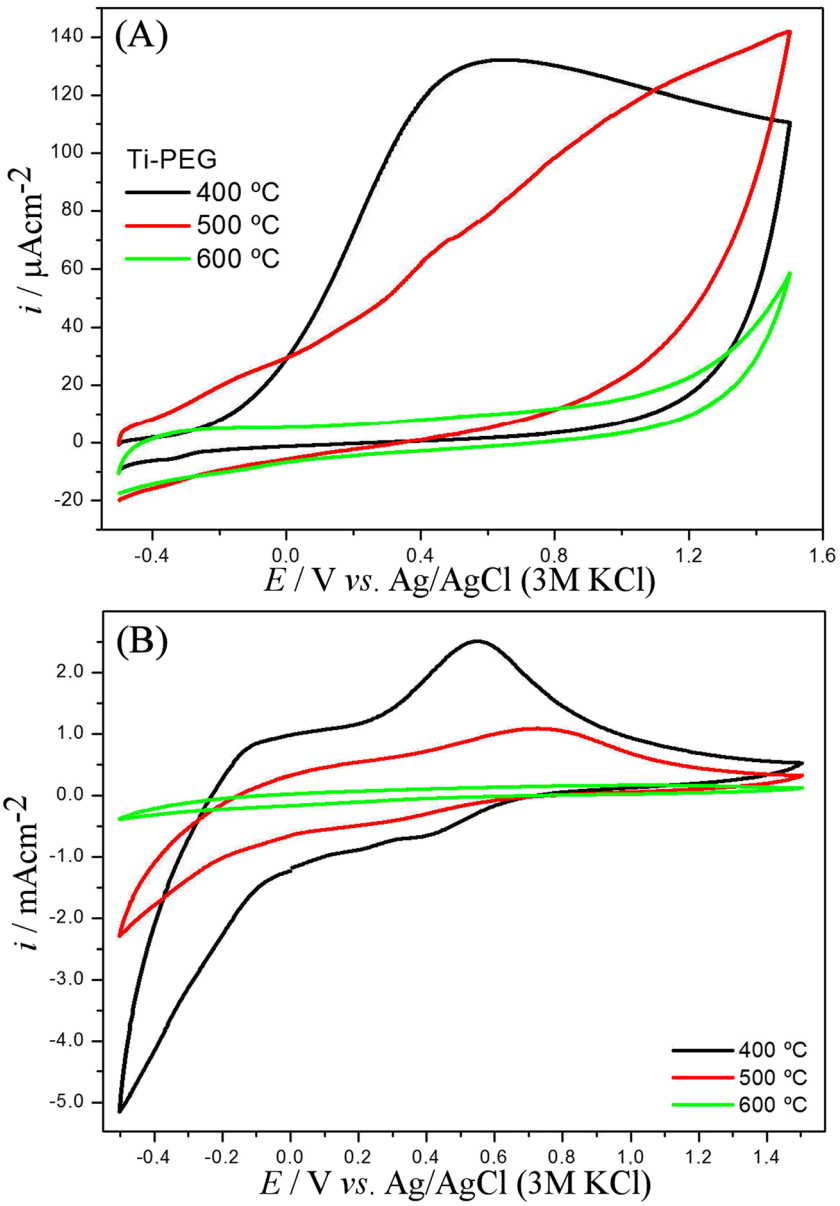

Fig. 6 **a** Cyclic voltammograms (0.5 mol dm^{-3} Na_2SO_4, third potential cycle shown; scan rate 20 mV s^{-1}) comparing titanium electrodes produced with only PEG300 at 400, 500, and 600 °C. **b** As above, but for electrodes coated with nano-V_2O_5

additional oxide layers forming at higher temperature on the titanium substrate. A comparison of the voltammetric responses of nano-V_2O_5 films and those for $BiVO_4$ films is shown in Fig. 4c–e. The current responses are similar which may indicate a relatively similar surface redox chemistry of these materials. Photocurrents for nano-V_2O_5 on titanium remain very low (*vide infra*).

Bi^{3+} impregnation and restructuring of nano-V_2O_5 films on titanium substrates

Given the similarity of the surface redox chemistry of nano-V_2O_5 and $BiVO_4$, it is interesting to react/impregnate the surface with aqueous Bi^{3+}. Figure 7 shows SEM images of nano-V_2O_5 samples obtained at different temperatures (400, 500, and 600 °C) after 2 h of impregnation in 10 mM $Bi(NO_3)_3$ in 10 mM HNO_3 and with 2 h of additional calcination at same temperature (400, 500, and 600 °C).

Perhaps surprisingly, after impregnation with Bi^{3+}, the surfaces of the samples are changed and even the 400 °C sample has been transformed into a crystalline material, rod-shaped with 10 μm and more length. Also, for the samples obtained at 500 °C, there are elongated crystals, but for the sample obtained at 600 °C, more globular structures are formed with the underlying nano-V_2O_5 crystals still visible. The formation of the crystals is likely to occur during impregnation in aqueous

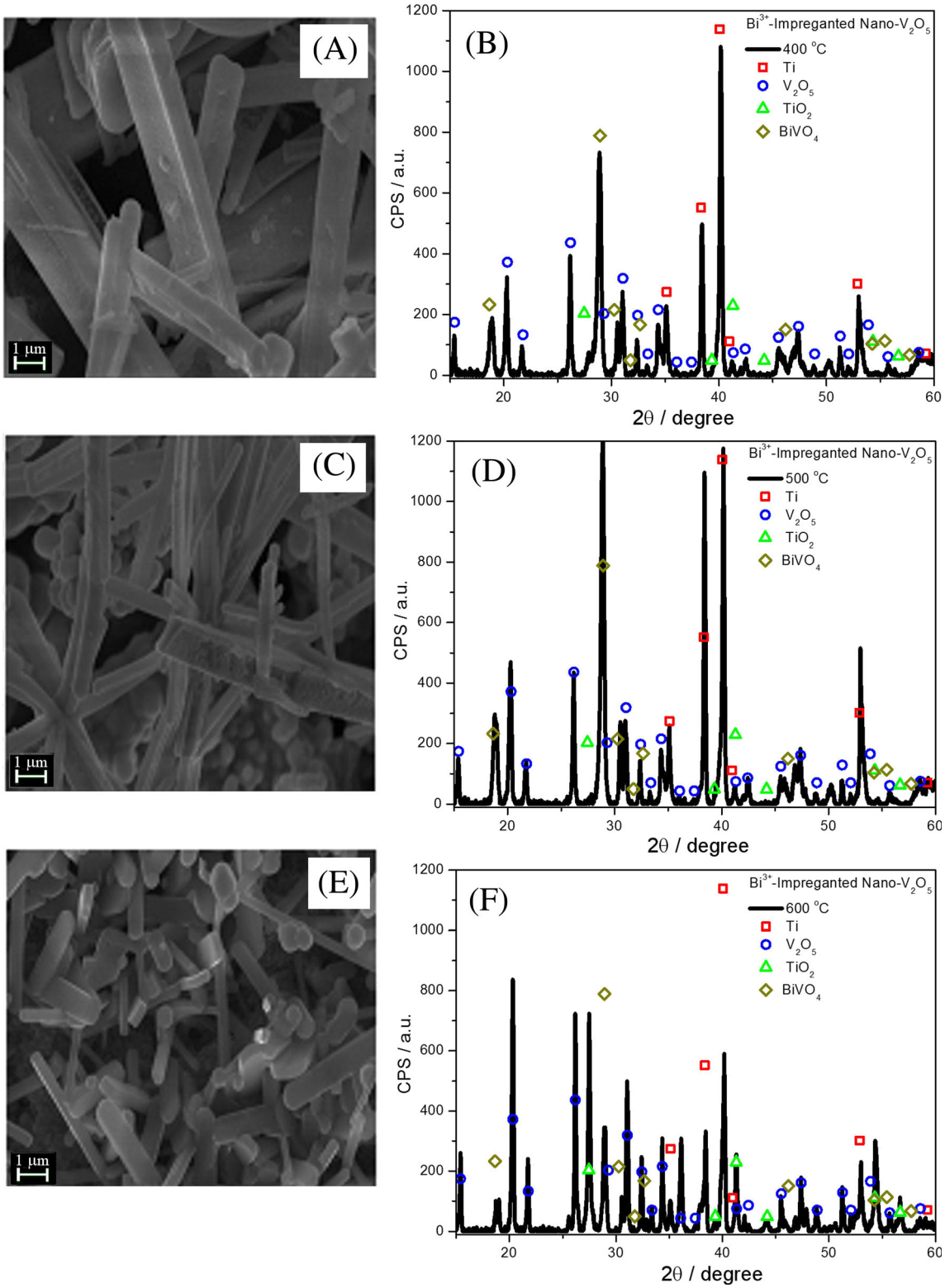

Fig. 7 **a**, **c**, **e** Scanning electron microscopy (SEM) images of "two-step" nano-V_2O_5 films obtained at calcination temperatures of 400, 500, and 600 °C. **b**, **d**, **f** XRD data for 400, 500, and 600 °C samples

solution where the high surface area nano-V_2O_5 is more reactive leading to a more rapid conversion. EDS spectra were obtained at 15-KeV electron beam power (Table 2) and suggest that the highest Bi level is in the sample obtained at 500 °C. However, the atom percentages of Bi in the films low (see Table 1) giving Bi/

Table 2 Energy-dispersive fluorescence (EDS) data obtained under SEM conditions with 15-KeV electron beam energy for "two-step" $BiVO_4$ samples on titanium

T (°C)	Region	At%			
		V	Bi	O	Ti
400	1	8.88	1.82	78.14	11.16
	2	8.90	1.75	78.72	10.63
	3	9.24	1.92	78.35	10.49
	Average	9.01	1.83	78.40	10.76
500	1	13.14	4.42	75.08	7.36
	2	14.72	7.00	70.05	8.23
	3	9.76	3.11	73.84	13.29
	Average	12.54	4.84	72.99	9.63
600	1	7.47	0.40	87.13	5.01
	2	6.80	0.39	85.98	6.83
	3	7.49	0.53	86.79	5.21
	Average	7.25	0.44	86.63	5.68

V ratios of 0.20, 0.39, and 0.06 at temperatures of 400, 500, and 600 °C, respectively. XRD analysis (Fig. 7b, d, f) confirms a higher level of $BiVO_4$ in samples prepared at 400 and 500 °C.

Voltammetric study of the two-step $BiVO_4$ film electrodes (2-h impregnation with Bi^{3+} at 20 °C followed by calcination, Fig. 8) reveals only minor changes in the reduction and oxidation responses. It is likely that the change in the "dark" redox behavior remains insignificant due to the similarity of nano-V_2O_5 and $BiVO_4$ surface processes. However, significant changes in photocurrents are observed (*vide infra*).

Photovoltammetry for Bi^{3+}-impregnated nano-V_2O_5 on titanium substrates

Photocurrent responses for two-step $BiVO_4$ on titanium substrates are shown in Fig. 9. In the presence of pulsed light, much improved photocurrents are seen with

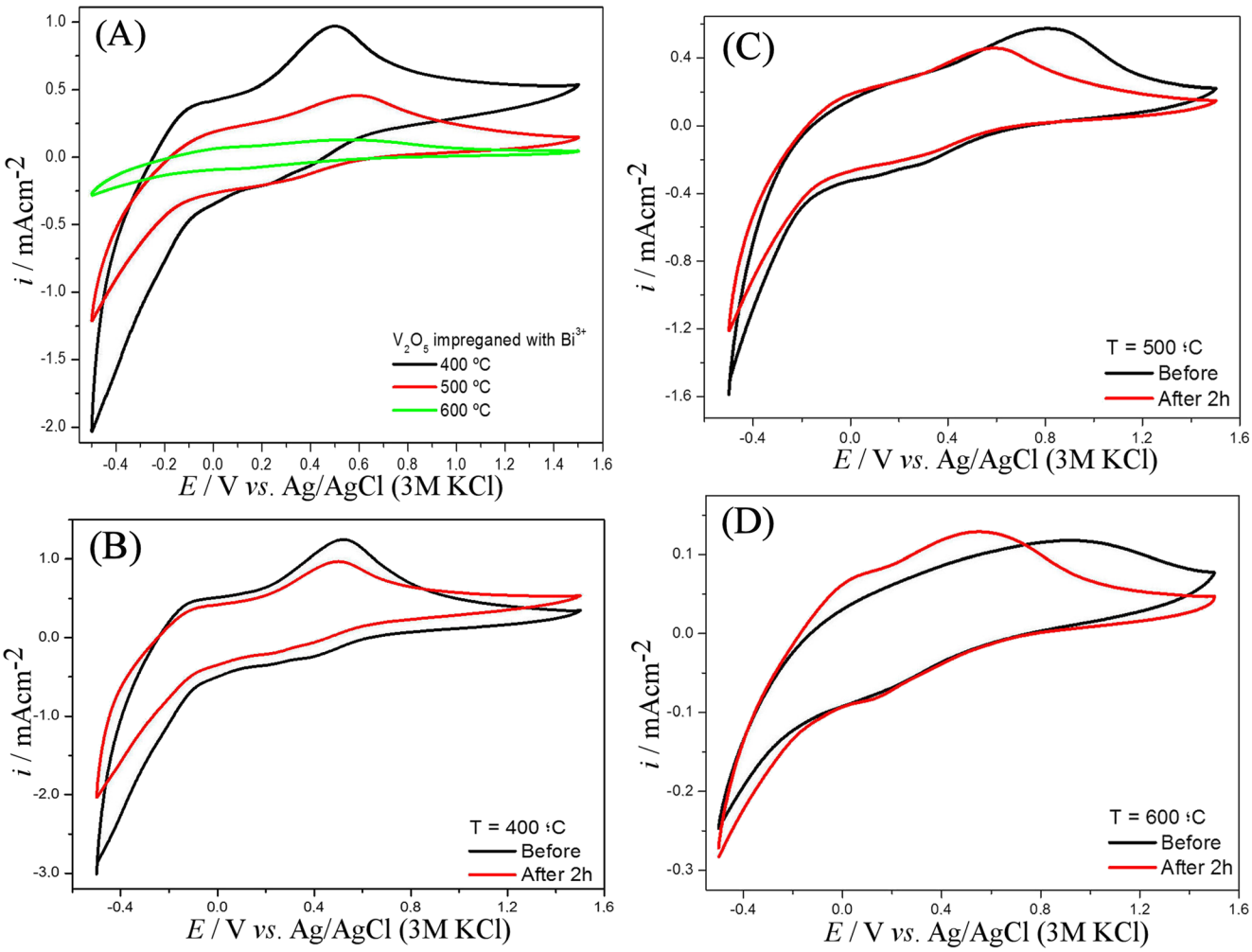

Fig. 8 **a** Cyclic voltammograms (0.5 mol dm^{-3} Na_2SO_4, third potential cycle shown; scan rate 20 mV s^{-1}) comparing "two-step" $BiVO_4$ films (2-h impregnation with Bi^{3+} at 20 °C followed by calcination) on titanium electrodes produced at 400, 500, and 600 °C. **b**–**d** As above, comparing two-step $BiVO_4$ and nano-V_2O_5 for samples prepared at temperatures of **b** 400, **c** 500, and **d** 600 °C

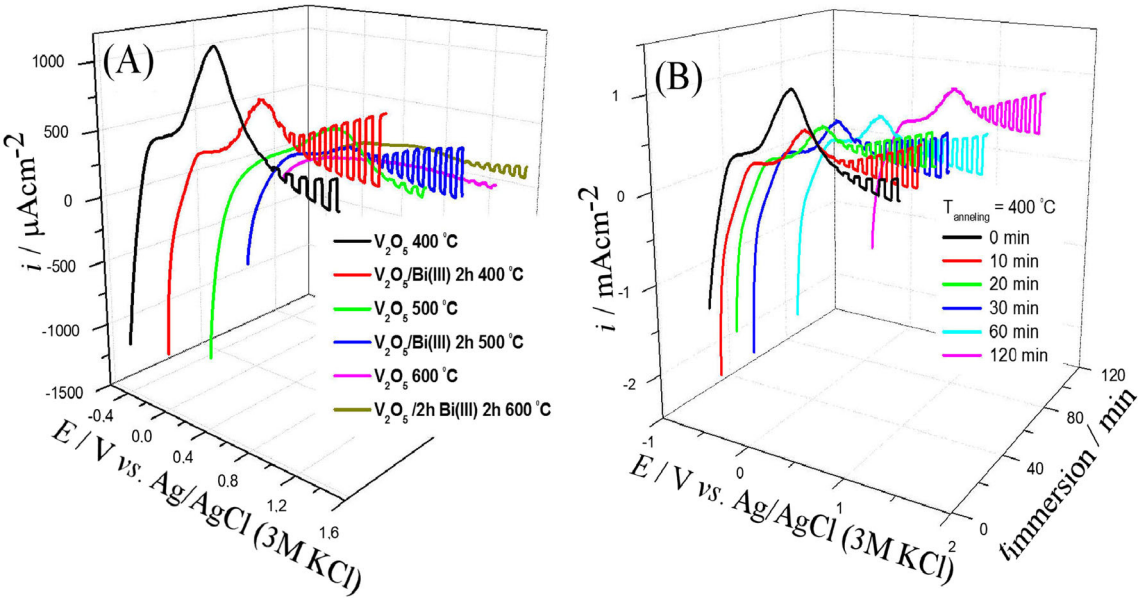

Fig. 9 **a** Linear scan voltammograms (0.5 mol dm^{-3} Na_2SO_4, light pulses with x s off and x s on, scan rate 20 mV s^{-1}) comparing photocurrents for nano-V_2O_5 and for "two-step" $BiVO_4$ films (2-h impregnation with Bi^{3+} at 20 °C followed by calcination) on titanium electrodes produced at 400, 500, and 600 °C. **b** As above, but for "two-step" $BiVO_4$ produced at 400 °C as a function of impregnation time

significant responses (ca. 300 μA cm^{-2} at 1.0 V versus Ag/AgCl (KCl 3 M)) in particular for 400 °C calcined films. This level of photocurrent is similar to that for $BiVO_4$ on ITO substrates [28] (although below that of high quality $BiVO_4$ electrodes) and consistent with a high level of light to current conversion. Samples prepared at higher calcination temperature remain poor in terms of photocurrents. Some underlying dark current features are believed to be related to the negative starting point of the potential scans. Figure 9b shows the effect of the impregnation time on the photocurrents. Even shorter impregnation times of only 10 min result in samples with good photoefficiency.

Conclusions

It has been shown that PEG-based synthesis of nano-V_2O_5 on titanium substrates is readily achieved with well-formed nanocrystalline materials forming at elevated temperatures (at 600 °C). Although these materials are not significantly photoactive a simple Bi^{3+} impregnation step followed by mild annealing (at 400 °C) has been shown to convert the film on the titanium substrate into an effective photoanode with typically up to 0.3 mA cm^{-2} (at 1.0 V vs Ag/AgCl (KCl 3 M)) at 0.1-W cm^{-2} xenon lamp radiation. Therefore, cheap and high melting titanium metal substrates can be employed beneficially to make photoactive $BiVO_4$ devices.

Acknowledgments L.H.M. and F.M. thank CAPES (PVE 71/2013) and FAPESP (2013/07296-2) and CNPq (472384/2012-0) for financial support.

References

1. Lewerenz HJ, Peter L (eds) (2013) Photoelectrochemical water splitting: materials, processes and architectures. RSC Publishing, Cambridge
2. Nowotny J (2012) Oxide semiconductors for solar energy conversion: titanium dioxide. CRC Press, Boca Raton
3. Li ZS, Luo WJ, Zhang ML, Feng JY, Zou ZG (2013) Photoelectrochemical cells for solar hydrogen production: current state of promising photoelectrodes, methods to improve their properties, and outlook. Energy Environ Sci 6:347–370
4. Xie SL, Zhai T, Zhu YJ, Li W, Qiu RL, Tong YX, Lu XH (2014) NiO decorated Mo:$BiVO_4$ photoanode with enhanced visible-light photoelectrochemical activity. Internat J Hydrogen Energy 39: 4820–4827
5. Park Y, McDonald KJ, Choi KS (2013) Progress in bismuth vanadate photoanodes for use in solar water oxidation. Chem Soc Rev 42:2321–2337
6. Wang M, Liu Q, Che YS, Zhang LF, Zhang D (2013) Characterization and photocatalytic properties of N-doped $BiVO_4$ synthesized via a sol–gel method. J Alloys Compounds 548:70–76
7. Li DZ, Wang WZ, Jiang D, Zheng YL, Li XM (2015) Surfactant-free hydrothermal fabrication of monoclinic $BiVO_4$ photocatalyst with oxygen vacancies by copper doping. RSC Adv 5:14374–14381
8. Zhou L, Wang WZ, Liu SW, Zhang LS, Xu HL, Zhu W (2006) A sonochemical route to visible-lightdriven high-activity $BiVO_4$ photocatalyst. J Mol Catal A-Chem 252:120–124
9. Dunkle SS, Helmich RJ, Suslick KS (2009) $BiVO_4$ as a visible-light photocatalyst prepared by ultrasonic spray pyrolysis. J Phys Chem C 113:11980–11983

10. Osterloh FE (2013) Inorganic nanostructures for photoelectrochemical and photocatalytic water splitting. Chem Soc Rev 42:2294–2320
11. Wan YB, Wang SH, Luo WH, Zhao LH (2012) Impact of Preparative pH on the Morphology and Photocatalytic Activity of BiVO4. Internat J Photoenergy 392865
12. Jeong HW, Jeon TH, Jang JS, Choi W, Park H (2013) Strategic modification of $BiVO_4$ for improving photoelectrochemical water oxidation performance. J Phys Chem C 117:9104–9112
13. Jo JW, Jang JW, Kong KJ, Kang HJ, Kim JY, Jun H, Parmar KPS, Lee JS (2012) Phosphate doping into monoclinic $BiVO_4$ for enhanced photoelectrochemical water oxidation activity. Angew Chem Internat Ed 51:3147–3151
14. Kwolek P, Pilarczyk K, Tokarski T, Lewandowska K, Szacilowski K (2014) $Bi_xLa_{1-x}VO_4$ solid solutions: tuning of electronic properties via stoichiometry modifications. Nanoscale 6:2244–2254
15. Ye H, Park HS, Bard AJ (2011) Screening of electrocatalysts for photoelectrochemical water oxidation on W-doped $BiVO_4$ photocatalysts by scanning electrochemical microscopy. J Phys Chem C 115:12464–12470
16. Zhang K, Shi XJ, Kim JK, Park JH (2012) Photoelectrochemical cells with tungsten trioxide/Modoped $BiVO_4$ bilayers. Phys Chem Chem Phys 14:11119–11124
17. Jeon TH, Choi W, Park H (2011) Cobalt-phosphate complexes catalyze the photoelectrochemical water oxidation of $BiVO_4$ electrodes. Phys Chem Chem Phys 13:21392–21401
18. Choi SK, Choi W, Park H (2013) Solar water oxidation using nickel-borate coupled $BiVO_4$ photoelectrodes. Phys Chem Chem Phys 15:6499–6507
19. Cha HG, Choi KS (2015) Combined biomass valorization and hydrogen production in a photoelectrochemical cell. Nature Chem 7: 328–333
20. Cameron PJ, Peter LM (2005) How does back-reaction at the conducting glass substrate influence the dynamic photovoltage response of nanocrystalline dye-sensitized solar cells? J Phys Chem B 109:7392–7398
21. Eisenberg D, Ahn HS, Bard AJ (2014) Enhanced photoelectrochemical water oxidation on bismuth vanadate by electrodeposition of amorphous titanium dioxide. J Amer Chem Soc 136:14011–14014
22. Chen SY, Wang LW (2012) Thermodynamic oxidation and reduction potentials of photocatalytic semiconductors in aqueous solution. Chem Mater 24:3659–3666
23. Nakata K, Fujishima A (2012) TiO_2 photocatalysis: design and applications. J Photochem Photobiol C-Photochem Rev 13:169–189
24. Xie MZ, Fu XD, Jing LQ, Luan P, Feng YJ, Fu HG (2014) Long-lived, visible-light-excited charge carriers of $TiO_2/BiVO_4$ nanocomposites and their unexpected photoactivity for water splitting. Adv Energy Mater 4:1300995
25. Xie MZ, Feng YJ, Fu XD, Luan P, Jing LQ (2015) Phosphate-bridged TiO_2-$BiVO_4$ nanocomposites with exceptional visible activities for photocatalytic water splitting. J Alloys Comp 631:120–124
26. Huo TY, Zhang XF, Dong XL, Zhang XX, Ma C, Wang GW, Ma HC, Xue M (2014) Photonic crystal coupled porous $BiVO_4$ hybrid for efficient photocatalysis under visible light irradiation. J Mater Chem A 2:17366–17370
27. Ho-Kimura S, Moniz SJA, Handoko AD, Tang JW (2014) Enhanced photoelectrochemical water splitting by nanostructured $BiVO_4$-TiO_2 composite electrodes. J Mater Chem A 2:3948–3953
28. Mascaro LH, Pockett A, Mitchels JM, Peter LM, Cameron PJ, Celorrio V, Fermin DJ, Sagu JS, Wijayantha KGU, Kociok-Kohn G, Marken F (2015) One-step preparation of the $BiVO_4$ film photoelectrode. J Solid State Electrochem 19:31–35
29. Haber J, Nowak P (1995) A catalysis related electrochemical study of the V_2O_5/TiO_2 (rutile) system. Langmuir 11:1024–1032